Trans Jpn Soc Med Biol Eng
47(1) : 1-6, 2009

CONTRIBUTION

Physical Parameter Identification of Uniform Rheological Deformation Based on FE Simulation

Zhongkui WANG,* Kazuki NAMIMA,* Shinichi HIRAI*

Abstract Human tissues and organs often exhibit rheological behaviors during their deformation. For surgery simulation and human modeling, we have to identify physical parameters of such deformation in advance. In this paper, we propose an approach to estimate the physical parameters of uniform rheological deformation based on 2D/3D finite element (FE) model simulation. At first, the FE dynamic model was described and simulations were conducted with initial parameters. Then, the identification method was proposed according to analysis of deformation behavior. Finally, identification results were shown and their validity was evaluated by comparing identified parameters and initial ones. This method can be extended to visco-elastic and layered rheological deformation.

Keywords : identification, rheological deformation, physical parameter.

1. Introduction

Modeling of deformable soft objects is being applied to medical engineering, including human modeling, surgical simulation, and minimally invasive surgery. In surgical simulation, precise model of human tissues or organs are required to describe and predict the interaction between external forces or loads and deformation [1, 2]. Then, in order to reduce accident risks, a surgical training can be done sufficiently and properly before the actual surgery was carried out. In addition, to perform minimally invasive surgery, a needle insertion manipulated was commonly employed in clinical treatments. A precise model of the target object with essential properties is necessary for the precise control of the needle [3]. The simulation models of such objects have been intensively studied since late 80's and many methods had already been proposed to describe the deformation behavior of soft objects, such as: the mass-spring-damper method (MSD) [4], the finite difference method (FDM) [5], the boundary element method (BEM) [6], and the finite element method (FEM) [7]. However, all of these include important physical parameters which must be available before simulation. Unfortunately, there are little useful data can be obtained to describe these parameters until now.

In recent years, some methods had already been proposed to estimate physical parameters of soft objects. The classification of these methods can be simply described as **Fig. 1**. First of all, it can be roughly divided into two categories. The first one is deformation observation and iterative simulation. FE analysis is iterated with updated physical parameters until the difference between the displacements observed from images and calculated by FEM is minimized [8]. The Extended Kalman Filter (EKF) was utilized as estimator to optimize an objective function and a CCD camera or an ultrasonic device was employed to measure displacements [9, 10]. This method can easily take both nonlinear deformation and multi-layer structure into account and it works well to deal with the object with one parameter, for example the Young's modulus. But it will encounter problems in deformation with more than one parameter. One probably can get more than one set of identification results depend on same deformation behavior. It is because that all parameters, in multi-parameter deformation, will interact with each other and contribute to the deformation. There must be more than one set of parameters can satisfy the final deformation during iterations. This problem can be solved by introducing various loading patterns and force boundary conditions [11].

The second category is theoretical analysis which tends

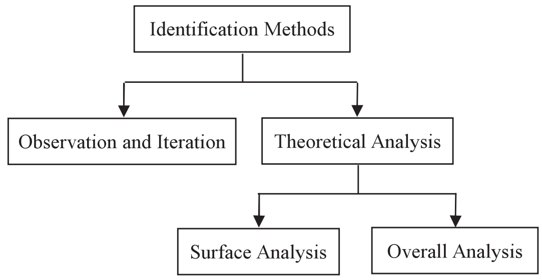

Fig. 1 Classification of identification methods.

Presented at the Symposium on Biomedical Engineering 2008, Osaka, September 2008.
Received July 29, 2008; revised October 1, 2008, January 7, 2009.
* Dept. of Robotics, Ritsumeikan University

to estimate the parameters by using the relationship between force and displacement of deformation based on elastic or inelastic theory. Furthermore, this category also can be divided into two subcategories. The first one called surface analysis which only uses displacement and force on the surface of object. A constant force was imparted on object surface by an air-jet and displacements of the surface were measured by high speed camera [12, 13]. Then, physical parameters can be estimated by analyzing the relationship between displacement and force. Comparing to other method, lesser measurable data are required in this method. Unfortunately, it is difficult to use this method in layered soft objects since only surface deformation data are available. The second subcategory is overall analysis. FE method was employed to establish dynamic model of deformation behavior, and displacements of all nodal points were measured by using CT or MRI device. Then, the parameters can be identified based on theoretical analysis of force and displacement [14, 15]. From above description, we can know that this method needs more measurable data. But it can be used not only in multi-parameter soft object deformation but also in both uniform and layered deformation. Moreover, along with the development of MRI and image processing technique, it will become more and more convenient to obtain inner displacements of object.

So far, related works in this field mainly focus on elastic or viscoelastic object [16, 17]. There are only few papers can be found working on rheological deformation [18, 19]. Our previous work had already developed an FE model for simulating linear rheological deformation [20] and an approach was also proposed to identify the physical parameters of rheological deformation based on 1D FE model simulation [21]. In this paper, we extend this method to 2D/3D rheological deformation. It belongs to the second subcategory according to above classification. In next section, 2D/3D FE dynamic model is presented and simulation results are given. Then, identification method is proposed based on theoretical analysis and identification results are presented in Section 3. In Section 4, we give a few conclusions and suggest future works.

2. Dynamic Model and Simulation

2·1 FE Dynamic Model

Depending on the deformation behavior in response to applied external force, deformable objects can be divided into three categories: viscoelastic, plastic, and rheological objects. Suppose that an object has a natural shape, as shown in **Fig. 2** (a). Applying external force, the object deformed as shown in Fig. 2 (b). After external force is removed, viscoelastic objects return to the original shape and there is no residual deformation, as shown in Fig. 2 (c). Plastic objects remain all the deformation and there is no recovered deformation, as shown in Fig. 2 (d). However, rheological objects partially remain the deformation but not all, as shown in Fig. 2 (e).

Rheological object can be described by three-element model which is a serial connection of a Voigt model and a viscous element. The 3D FE mesh used in this paper and

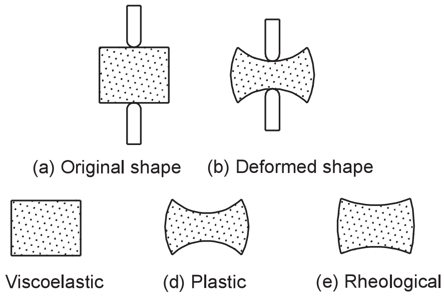

Fig. 2 Deformation classification of soft objects.

three-element model as illustrated in **Fig. 3**. This FE model consists of 5 × 5 × 5 mass points. There are totally 64 parallelepipeds and each of them consists of 6 identical tetrahedrons. A three-element model is attached on each tetrahedron. In 2D/3D dynamic model, we assume that deformation property is isotropic and linear. Rheological deformation of each tetrahedron is characterized by six parameters: λ^{ela}, μ^{ela}, λ_1^{vis}, μ_1^{vis}, λ_2^{vis}, μ_2^{vis}. The first two are Lamé's constants, which describe elastic deformation. The next two describe viscosity and the last two show plasticity. In elasticity theory [22], the Lamé's constants λ^{ela}, μ^{ela} can be described by Young's modulus E and Poisson's ratio γ as shown in Eq. 1. For the sake of simplicity, we assume that the other four parameters λ_1^{vis}, μ_1^{vis}, λ_2^{vis}, μ_2^{vis} have the same form with Lamé's constants as defined in Eq. 1, where c_1 and c_2 denote viscosity of two viscous elements respectively. These four physical parameters E, c_1, c_2, and γ will be employed as input in simulation and output in identification.

$$\lambda^{ela}=\frac{E\cdot\gamma}{(1+\gamma)(1-2\gamma)},\ \lambda_1^{vis}=\frac{c_1\cdot\gamma}{(1+\gamma)(1-2\gamma)},\ \lambda_2^{vis}=\frac{c_2\cdot\gamma}{(1+\gamma)(1-2\gamma)},$$
$$\mu^{ela}=\frac{E}{2(1+\gamma)},\ \mu_1^{vis}=\frac{c_1}{2(1+\gamma)},\ \mu_2^{vis}=\frac{c_1}{2(1+\gamma)}. \quad (1)$$

Then, dynamic equations of 2D/3D rheological deformation used in this paper can be described by a set of differential equations as follows:

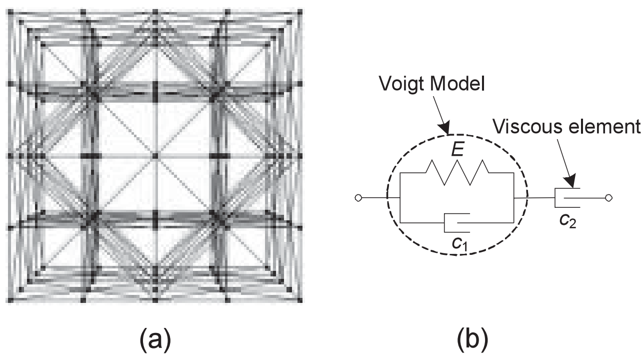

Fig. 3 3D FE mesh and three element model. (a) FE mesh includes 125 mass points, 64 parallelepipeds and 384 tetrahedrons. (b) Three-element model which can be employed to describe linear rheological deformation.

$$
\begin{bmatrix}
\mathbf{I} & & & & & & \\
 & \mathbf{M} & -\mathbf{A} & -\mathbf{B} & -\mathbf{C} & & \\
 & -\mathbf{A}^{\mathrm{T}} & & & & & \\
 & -\mathbf{B}^{\mathrm{T}} & & & & & \\
 & -\mathbf{C}^{\mathrm{T}} & & & & & \\
 & -\frac{\lambda_1^{\mathrm{vis}}\lambda_2^{\mathrm{vis}}}{\lambda_1^{\mathrm{vis}}+\lambda_2^{\mathrm{vis}}} & & & & \mathbf{I} & \\
 & -\frac{\mu_1^{\mathrm{vis}}\mu_2^{\mathrm{vis}}}{\mu_1^{\mathrm{vis}}+\mu_2^{\mathrm{vis}}} & & & & & \mathbf{I}
\end{bmatrix}
\begin{bmatrix}
\dot{\mathbf{u}}_{\mathrm{N}} \\ \dot{\mathbf{v}}_{\mathrm{N}} \\ \lambda_{\mathrm{A}} \\ \lambda_{\mathrm{B}} \\ \lambda_{\mathrm{C}} \\ \dot{\boldsymbol{\Omega}}_{\lambda} \\ \dot{\boldsymbol{\Omega}}_{\mu}
\end{bmatrix}
=
\begin{bmatrix}
\mathbf{v}_{\mathrm{N}} \\
-\mathbf{J}_{\lambda}\boldsymbol{\Omega}_{\lambda}-\mathbf{J}_{\mu}\boldsymbol{\Omega}_{\mu} \\
\mathbf{A}^{\mathrm{T}}(2\omega\mathbf{v}_{\mathrm{N}}+\omega^2\mathbf{u}_{\mathrm{N}}) \\
2\omega(\mathbf{B}^{\mathrm{T}}\mathbf{v}_{\mathrm{N}}-\dot{d}(t))+\omega^2(\mathbf{B}^{\mathrm{T}}\mathbf{u}_{\mathrm{N}}-d(t)) \\
\mathbf{C}^{\mathrm{T}}(2\omega\mathbf{v}_{\mathrm{N}}+\omega^2\mathbf{u}_{\mathrm{N}}) \\
-\frac{\lambda^{\mathrm{ela}}}{\lambda_1^{\mathrm{vis}}+\lambda_2^{\mathrm{vis}}}(\boldsymbol{\Omega}_{\lambda}-\lambda_2^{\mathrm{vis}}\mathbf{v}_{\mathrm{N}}) \\
-\frac{\mu^{\mathrm{ela}}}{\mu_1^{\mathrm{vis}}+\mu_2^{\mathrm{vis}}}(\boldsymbol{\Omega}_{\mu}-\mu_2^{\mathrm{vis}}\mathbf{v}_{\mathrm{N}})
\end{bmatrix}
\quad (2)
$$

where M is the inertia matrix, **A**, **B** and **C** are three constraint matrices, $d(t)$ is displacement constraint function, $\mathbf{u}_{\mathrm{N}}=[x_1, y_1, z_1, \cdots\cdots, x_{125}, y_{125}, z_{125}]^{\mathrm{T}}$ and $\mathbf{v}_{\mathrm{N}}=\dot{\mathbf{u}}_{\mathrm{N}}$ are displacement vector and velocity vector of every point, $\lambda_{\mathbf{A}}$, $\lambda_{\mathbf{B}}$ and λ_{C} are Lagrange multiplier vectors which denote constraint forces on bottom surface and top surface respectively, ω denotes a predetermined angular frequency, $\mathbf{J}_{\lambda}$ and $\mathbf{J}_{\mu}$ are two connection matrixes determined by geometric quantities alone. Vectors $\boldsymbol{\Omega}_{\lambda}$ and $\boldsymbol{\Omega}_{\mu}$ are defined as follows to simplify expression of force[23]:

$$
\begin{aligned}
\boldsymbol{\Omega}_{\lambda} &= \int_0^t \frac{\lambda^{\mathrm{ela}}\lambda_2^{\mathrm{vis}}}{\lambda_1^{\mathrm{vis}}+\lambda_2^{\mathrm{vis}}} e^{-\frac{\lambda^{\mathrm{ela}}}{\lambda_1^{\mathrm{vis}}+\lambda_2^{\mathrm{vis}}}(t-t')}\left(\dot{\mathbf{u}}_{\mathrm{N}}+\frac{\lambda_1^{\mathrm{vis}}}{\lambda^{\mathrm{ela}}}\ddot{\mathbf{u}}_{\mathrm{N}}\right)(t')\,\mathrm{d}t' \\
\boldsymbol{\Omega}_{\mu} &= \int_0^t \frac{\mu^{\mathrm{ela}}\mu_2^{\mathrm{vis}}}{\mu_1^{\mathrm{vis}}+\mu_2^{\mathrm{vis}}} e^{-\frac{\mu^{\mathrm{ela}}}{\mu_1^{\mathrm{vis}}+\mu_1^{\mathrm{vis}}}(t-t')}\left(\dot{\mathbf{u}}_{\mathrm{N}}+\frac{\mu_1^{\mathrm{vis}}}{\mu^{\mathrm{ela}}}\ddot{\mathbf{u}}_{\mathrm{N}}\right)(t')\,\mathrm{d}t'
\end{aligned}
\quad (3)
$$

A set of rheological forces applied to all nodal points are then simply described as[23]:

$$\mathbf{F} = \mathbf{J}_{\lambda}\boldsymbol{\Omega}_{\lambda}+\mathbf{J}_{\mu}\boldsymbol{\Omega}_{\mu} \quad (4)$$

2·2 Simulation of Rheological deformation

During simulation, we supposed that nodal points on bottom surface fixed on the ground. So, constraint matrix **A** used to restrict displacements of the bottom surface can be described as

$$
\mathbf{A}=\begin{bmatrix}
\mathbf{I}_{3\times3} & \cdots & \mathbf{0}_{3\times3} \\
\vdots & \ddots & \vdots \\
\mathbf{0}_{3\times3} & \cdots & \mathbf{I}_{3\times3} \\
\vdots & \ddots & \vdots \\
\mathbf{0}_{3\times3} & \cdots & \mathbf{0}_{3\times3}
\end{bmatrix}_{375\times75}
;\ \text{where } \mathbf{I}_{3\times3}=\begin{bmatrix}1&0&0\\0&1&0\\0&0&1\end{bmatrix},\ \mathbf{0}_{3\times3}=\begin{bmatrix}0&0&0\\0&0&0\\0&0&0\end{bmatrix}
$$

Deformation process during simulation is divided into three steps. At first, we give a constant velocity to *y*-axis displacements of nodal points on the top surface from time 0 to time t_p and we call this period push phase. Then, we keep the displacements of these points from time t_p to time t_k and we call it keep phase. Finally we release this constraint after time t_k and we call it release phase. This displacement constraint function can be described by following equations:

$$
\begin{cases}
d(t)=\dfrac{\mathrm{d}}{\mathrm{t_p}}t; & 0\le t\le \mathrm{t_p} \\
d(t)=\mathrm{d}; & \mathrm{t_p}<t\le \mathrm{t_p}+\mathrm{t_k}
\end{cases}
\quad (5)
$$

where d is constant displacement of points on the top surface.

Then, the constraint matrix **B** used to restrict *y*-axis displacements of the top surface was give as

$$
\mathbf{B}=\begin{bmatrix}
\mathbf{0}_{3\times3} & \cdots & \mathbf{0}_{3\times3} \\
\vdots & \ddots & \vdots \\
\mathbf{b}_{3\times3} & \cdots & \mathbf{0}_{3\times3} \\
\vdots & \ddots & \vdots \\
\mathbf{0}_{3\times3} & \cdots & \mathbf{b}_{3\times3}
\end{bmatrix}_{375\times75}
;\ \text{where } \mathbf{b}_{3\times3}=\begin{bmatrix}0&0&0\\0&1&0\\0&0&0\end{bmatrix}
$$

We supposed again that *x*-axis and *z*-axis displacements of nodal points on the top surface do not change during simulation. So, constraint matrix **C** can be described as

$$
\mathbf{C}=\begin{bmatrix}
\mathbf{0}_{3\times3} & \cdots & \mathbf{0}_{3\times3} \\
\vdots & \ddots & \vdots \\
\mathbf{c}_{3\times3} & \cdots & \mathbf{0}_{3\times3} \\
\vdots & \ddots & \vdots \\
\mathbf{0}_{3\times3} & \cdots & \mathbf{c}_{3\times3}
\end{bmatrix}_{375\times75}
;\ \text{where } \mathbf{c}_{3\times3}=\begin{bmatrix}1&0&0\\0&0&0\\0&0&1\end{bmatrix}
$$

Dynamic FE model given in Eq. 2 can be employed to simulate linear rheological deformation. In this paper, we perform two simulations with different physical parameters, shown in **Table 1**. The initial shape of object can be found in Fig. 3, in which the length of each element between every two neighboring points is 0.01 m. The deformed shapes were shown in **Fig. 4**. Displacements of some nodal points and normal rheological forces are shown in **Fig. 5** and **Fig. 6**.

3. Identification Method

During the identification process, we supposed that we had already known the initial and final position of all nodal points and normal forces on bottom surface. These data can be easily measured by using CT or MRI device and force sensors in actual experiments.

There are 6 parameters in 2D/3D dynamic model given in Section 2. However, there are only four unknown

Table 1 Initial parameters in both simulations.

Parameters	E (Pa)	c_1 (Pa·s)	c_2 (Pa·s)	γ	d (m)	t_p (s)	t_k (s)
Case 1	8	5	40	0.43	0.006	120	120
Case 2	300	200	500	0.35	0.01	80	60

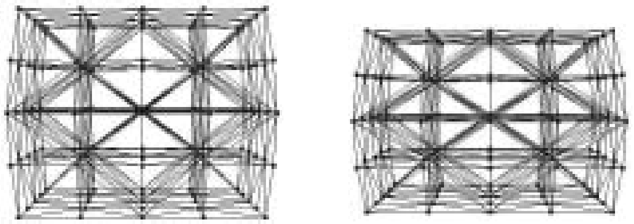

(a) Case 1 (b) Case 2

Fig. 4 Deformed shapes in both simulations. (a) Final deformation with parameters: $E = 8$ Pa, $c_1 = 5$ Pa·s, $c_2 = 40$ Pa·s, and $\gamma = 0.43$. (b) Final deformation with parameters: $E = 300$ Pa, $c_1 = 200$ Pa·s, $c_2 = 500$ Pa·s, and $\gamma = 0.35$.

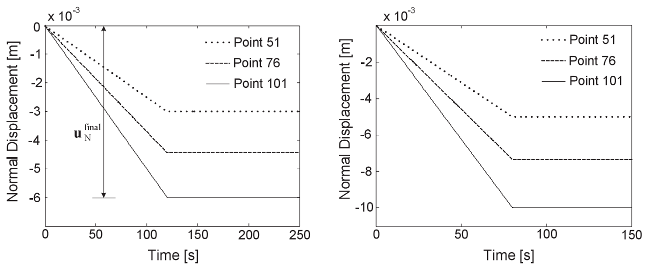

(a) Case 1 (b) Case 2

Fig. 5 Normal displacements of some nodal points in both simulations. In push phase, displacements of all points increase with a constant velocity. In keep phase, displacements keep constant and there is no displacements recovery after releasing.

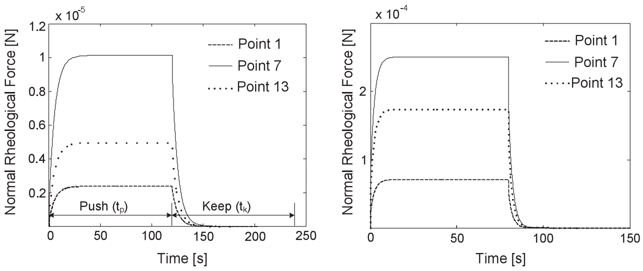

(a) Case 1 (b) Case 2

Fig. 6 Normal rheological forces on the bottom surface in both simulations. Rheological force increases quickly in push phase and converges to a constant value. In keep phase, rheological force decreases quickly to zero.

physical parameters need to be identified. Here we choose λ^{ela}, λ_1^{vis}, λ_2^{vis} and μ_2^{vis} as four independent parameters to present how to estimate them step by step. By taking time derivative of Eq. 4 and substituting Eq. 3 into it, we have

$$\begin{aligned}\dot{\mathbf{F}} &= \mathbf{J}_\lambda\dot{\boldsymbol{\Omega}}_\lambda+\mathbf{J}_\mu\dot{\boldsymbol{\Omega}}_\mu \\ &= -\frac{\lambda^{ela}}{\lambda_1^{vis}+\lambda_2^{vis}}\mathbf{J}_\lambda\boldsymbol{\Omega}_\lambda+\frac{\lambda^{ela}\lambda_2^{vis}}{\lambda_1^{vis}+\lambda_2^{vis}}\mathbf{J}_\lambda\dot{\mathbf{u}}_N+\frac{\lambda_1^{vis}\lambda_2^{vis}}{\lambda_1^{vis}+\lambda_2^{vis}}\mathbf{J}_\lambda\ddot{\mathbf{u}}_N, \\ &\quad -\frac{\mu^{ela}}{\mu_1^{vis}+\mu_2^{vis}}\mathbf{J}_\mu\boldsymbol{\Omega}_\mu+\frac{\mu^{ela}\mu_2^{vis}}{\mu_1^{vis}+\mu_2^{vis}}\mathbf{J}_\mu\dot{\mathbf{u}}_N+\frac{\mu_1^{vis}\mu_2^{vis}}{\mu_1^{vis}+\mu_2^{vis}}\mathbf{J}_\mu\ddot{\mathbf{u}}_N\end{aligned} \tag{6}$$

From Eq. 1, we know the coefficients of the first and fourth term in right side of Eq. 6 are equal to each other. Considering Eq. 4, above equation can be rewritten as below:

$$\dot{\mathbf{F}}+\frac{\lambda^{ela}}{\lambda_1^{vis}+\lambda_2^{vis}}\mathbf{F}=\frac{1}{\lambda_1^{vis}+\lambda_2^{vis}}(\lambda_2^{vis}\mathbf{J}_\lambda+\mu_2^{vis}\mathbf{J}_\mu)(\lambda^{ela}\dot{\mathbf{u}}_N+\lambda_1^{vis}\ddot{\mathbf{u}}_N), \tag{7}$$

Eq. 7 shows the relationship between rheological forces and displacements of all nodal points in 2D/3D deformation.

Now, let us consider deformation behavior in push phase. During this phase, the deformation velocity of every point on the top surface is constant. So, if this velocity is slow enough, we can ignore dynamic effect and treat the velocity of all nodal points as constant. According to Fig. 5, this velocity can be approximately denoted by $\mathbf{u}_N^{final}/t_p$. So we can get analytical expression of rheological force in push phase by solving Eq. 7.

$$\mathbf{F}_p(t)=\mathbf{F}(t_1)e^{\frac{\lambda^{ela}}{\lambda_1^{vis}+\lambda_2^{vis}}(t_1-t)}+(\lambda_2^{vis}\mathbf{J}_\lambda+\mu_2^{vis}\mathbf{J}_\mu)\frac{\mathbf{u}_N^{final}}{t_p}\left(1-e^{\frac{\lambda^{ela}}{\lambda_1^{vis}+\lambda_2^{vis}}(t_1-t)}\right) \tag{8}$$

where $F(t_1)$ is integral initial value of force data at time t_1 which should be close to time zero.

Then, we derive analytical expression of rheological force in keep phase where the velocity and acceleration of nodal points are all equal to zero. We can obtain rheological force in this phase by solving Eq. 7 with integral initial force $F(t_2)$.

$$\mathbf{F}_k(t)=\mathbf{F}(t_2)e^{\frac{\lambda^{ela}}{\lambda_1^{vis}+\lambda_2^{vis}}(t_2-t)} \tag{9}$$

where t_2 is integral initial time, which should be larger than but close to time t_p.

Let us pay more attention to keep phase. In this phase, displacements of all nodal points remain constants but rheological force decreases quickly, as shown in Fig. 6. This behavior is called force relaxation in stress analysis [24]. During force relaxation, the displacements produced by elastic part will translate to plastic part. In plastic part, rheological force can be described as below:

$$\mathbf{F}(t)=(\lambda_2^{vis}\mathbf{J}_\lambda+\mu_2^{vis}\mathbf{J}_\mu)\dot{\mathbf{u}}_N^{vis}(t) \tag{10}$$

where $\mathbf{u}_N^{vis}$ are displacements in plastic part. Thus, we can calculate displacements of elastic part at time t_p by integrating F_k from time t_p to time infinite.

$$\begin{aligned}(\lambda_2^{vis}\mathbf{J}_\lambda+\mu_2^{vis}\mathbf{J}_\mu)\mathbf{u}_N^{Voigt}(t_p) &= (\lambda_2^{vis}\mathbf{J}_\lambda+\mu_2^{vis}\mathbf{J}_\mu)\int_{t_p}^{\infty}\dot{\mathbf{u}}_N^{vis}(t)\,dt \\ &= \int_{t_p}^{\infty}\mathbf{F}_k(t)\,dt=\frac{\lambda_1^{vis}+\lambda_2^{vis}}{\lambda^{ela}}\mathbf{F}_k(t_p) \\ &= \frac{\lambda_1^{vis}+\lambda_2^{vis}}{\lambda^{ela}}\mathbf{F}_k^{\lambda}(t_p)+\frac{\mu_1^{vis}+\mu_2^{vis}}{\mu^{ela}}\mathbf{F}_k^{\mu}(t_p)\end{aligned} \tag{11}$$

where $\mathbf{u}_N^{Voigt}(t_p)$ are displacements in elastic part at time t_p. $\mathbf{F}_k^{\lambda}(t_p)$ and $\mathbf{F}_k^{\mu}(t_p)$ denote normal force and tangential force respectively, and subject to $\mathbf{F}_k^{\lambda}(t_p)+\mathbf{F}_k^{\mu}(t_p)=\mathbf{F}_k(t_p)$. Comparing left side and right side of Eq. 11, we have

$$\begin{aligned}\mathbf{J}_\lambda\mathbf{u}_N^{Voigt}(t_p) &= \frac{\lambda_1^{vis}+\lambda_2^{vis}}{\lambda^{ela}\lambda_2^{vis}}\mathbf{F}_k^{\lambda}(t_p), \\ \mathbf{J}_\mu\mathbf{u}_N^{Voigt}(t_p) &= \frac{\mu_1^{vis}+\mu_2^{vis}}{\mu^{ela}\mu_2^{vis}}\mathbf{F}_k^{\mu}(t_p).\end{aligned} \tag{12}$$

In elastic part, rheological force can be described as follows

$$\mathbf{F}(t)=(\lambda^{ela}\mathbf{J}_\lambda+\mu^{ela}\mathbf{J}_\mu)\mathbf{u}_N^{Voigt}(t)+(\lambda_1^{vis}\mathbf{J}_\lambda+\mu_1^{vis}\mathbf{J}_\mu)\dot{\mathbf{u}}_N^{Voigt}(t) \tag{13}$$

From Fig. 6 we know that the rheological force does not change around time t_p. This means that the displacements produced by this part should be constants, resulting that $\dot{\mathbf{u}}_N^{\mathrm{Voigt}}(t_p)$ equal to zero. By substituting Eq. 12 into Eq. 13, we have

$$\begin{aligned}\mathbf{F}_p(t_p) &= (\lambda^{\mathrm{ela}}\mathbf{J}_\lambda+\mu^{\mathrm{ela}}\mathbf{J}_\mu)\mathbf{u}_N^{\mathrm{Voigt}}(t)\\ &= \frac{\lambda_1^{\mathrm{vis}}+\lambda_2^{\mathrm{vis}}}{\lambda_2^{\mathrm{vis}}}\mathbf{F}_k^\lambda(t_p)+\frac{\mu_1^{\mathrm{vis}}+\mu_2^{\mathrm{vis}}}{\mu_2^{\mathrm{vis}}}\mathbf{F}_k^\mu(t_p)\\ &= \frac{\lambda_1^{\mathrm{vis}}+\lambda_2^{\mathrm{vis}}}{\lambda_2^{\mathrm{vis}}}\mathbf{F}_k(t_p)\end{aligned} \tag{14}$$

Now, we can estimate physical parameters analytically by solving Eq. 8, Eq. 9 and Eq. 14. Firstly, by substituting force data of some bottom points into Eq. 9 and using Least Square Method (LSM), we can compute the value of $\lambda^{\mathrm{ela}}/(\lambda_1^{\mathrm{vis}}+\lambda_2^{\mathrm{vis}})$. Then, this value along with force data on bottom points and displacements of all points were substituted into Eq. 8 and LSM was employed again to solve them, we then can have the value of λ_2^{vis} and μ_2^{vis}. Finally, the same computation was used to solve Eq. 14 and the value of $(\lambda_1^{\mathrm{vis}}+\lambda_2^{\mathrm{vis}})/\lambda_2^{\mathrm{vis}}$ can be obtained. Consequently, we can identify 4 physical parameters by some simple substitutions. Identification results can be found in **Table 2**.

4. Conclusions and Future Works

In this paper, we proposed a method to identify physical parameters of uniform rheological deformation base on 2D/3D FE model simulations. We discussed two deformation behaviors with different parameters and simulation results were given. Then, Identification method was proposed according to the analysis of rheological force and displacement. At last, this method was validated by identification results. From Section 3, we find that this method is easily applicable because just a few calculations were involved in the identification process as long as required data are known. These data include initial and final position of all nodal points which can be measured by CT or MRI device and normal rheological force on bottom surface which can be measured by force sensor. In addition, this method can be extended to elastic or visco-elastic deformation and layered non-uniform deformation.

In the future, experiments will be performed to validate our method and parameter identification for non-uniform rheological deformation will be done. Then, nonlinear behavior also should be taken into account in rheological deformation.

References

1. Yang H, Liu PX, Zhang JD: Modeling of needle insertion forces for surgical simulation. Proc. of the IEEE International Conference on Mechatronics & Automation, Niagara Falls, Canada, 2005, pp. 592–595.
2. Tillier Y, Paccini A, Durand-Reville M, Bay F, Chenot J-L: Three-dimensional finite element modeling for soft tissues surgery. Proc. of the 17th International Congress and Exhibition on Computer Assisted Radiology and Surgery, vol. 1256, London, UK, 2003, pp. 349–355.
3. Kobayashi Y, Okamoto J, Fujie MG: Physical properties of the liver for needle insertion control. Proc. of 2004 IEEE/RSJ International Conference on Intelligent Robots and Systems, vol. 3, Sendai, 2004, pp. 2960–2966.
4. Nogami R, Noborio H, Tomokuni S, Hirai S: A comparative study of rheology MSD models whose structures are lattice and truss. Proc. of 2004 IEEE/RSJ International Conference on intelligent Robots and Systems, vol. 4, Sendai, 2004, pp. 3809–3816.
5. Terzopoulos D, Platt J, Barr A, Fleischer K: Elastically deformable models. ACM SIGGRAPH Computer Graphics, Vol. 21, New York, 1987, pp. 205–214.
6. Monserrat C, Meier U, Alcaniz M, Chinesta F, Juan MC: A new approach for the real-time simulation of tissue deformations in surgery simulation. Comput methods Programs Biomed. **64**: 77–85, 2001.
7. Nielsen MB, Cotin S: Real-time volumetric deformable models for surgery simulation using finite elements and condensation. Comput Graphics Forum (Proc. Eurographics). **15**: 57–66, 1996.
8. Tada M, Nagai N, Maeno T: Material properties estimation of layered soft tissue based on MR observation and iterative FE simulation. Medical Image Computing and Computer-Assisted Intervention- MICCAI 2005, Springer Berlin/Heidelberg, Vol. 3750, pp. 633–640, 2005.
9. Hoshi T, Kobayashi Y, Kawamura K, Fujie MG: Developing an intra-operative methodology using the finite element method and the Extended Kalman Filter to identify the material parameters of an organ model. Proc of the 29th Annual International Conference of the IEEE EMBS, Lyon, 2007, pp. 469–474.
10. Hoshi T, Kobayashi Y, Fujie MG: Developing a method using the Extended Kalman Filter to identify the material parameters of deformation model of organ. Proc of the 2008 JSME Conference on Robotics and Mechatronics, Nagano, 2008, pp. 1A1–C18.
11. Augenstein KF, Cowan BR, LeGrice IJ, Neilsen PMF, Young AA: Method and apparatus for soft tissue material parameter estimation using tissue tagged magnetic resonance imaging. J Biomech Eng. **127**: 148–157, 2005.

Table 2 Identification results of both deformations.

Parameters		E (Pa)	c_1 (Pa·s)	c_2 (Pa·s)	γ
Case 1	Results	8.0126	4.9914	40.0069	0.4301
	Error (%)	0.158	0.172	0.017	0.023
Case 2	Results	300.2574	200.0617	500.3169	0.3502
	Error (%)	0.086	0.031	0.063	0.057

12. Tanaka N, Kaneko M: Direction dependent response of human skin. Proc of the 29th Annual International Conference of the IEEE EMBS, Lyon, 2007, pp. 1687–1690.
13. Tanaka N, Higashimori M, Kaneko M: Non-contact active sensing for viscoelastic tissue with coupling effect. Proc of the 2008 JSME Conference on Robotics and Mechatronics, Nagano, 2008, pp. 1P1–H10.
14. Endo K, Muramatsu J, Hirai S: Physical parameters identification of FE model through measurement of inner deformation. Proc of the 2007 JSME Conference on Robotics and Mechatronics, Akita, 2007, pp. 2A1–B04.
15. Endo K, Zhang PL, Hirai S, Tokumoto S: Identification of non-uniform physical parameters through measurement of inner deformation. The Third Joint Workshop on Machine Perception and Robotics, Kusatsu, 2007, Ps2.
16. Lioyd BA, Székely G, Harders M: Identification of spring parameters for deformable object simulation. IEEE Trans Visualization Comput Graphics. **13**: 1081–1094, 2007.
17. Ahn B, Kim J: An efficient soft tissue characterization method for haptic rendering of soft tissue deformation in medical simulation. Frontiers in the convergence of Bioscience and Information Technologies 2007, Jejudo, 2007, pp. 549–553.
18. Sharma MG: Rheological properties of large arteries. Proc, of the Fourteenth Annual Northeast Bioengineering Conference, Durham, 1988, pp. 175–177.
19. Ueda N, Hirai S, Tanaka HT: Extracting rheological properties of deformable objects with haptic vision. Proc of the 2004 IEEE International Conference on Robotics & Automation, Vol. 4, New Orleans, 2004, pp. 3902–3907.
20. Muramatsu J, Ikuta T, Hirai S: Validation of FE deformation models using ultrasonic and MR images. Proc. of the 9th International Conference on Control, Automation, Robotics and Vision, Singapore, 2006, pp. 1–6.
21. Wang ZK, Hirai S: Physical parameter identification of uniform rheological deformation through FE model simulation. Proc. of the 2008 JSME Conference on Robotics and Mechatronics, Nagano, 2008, pp. 1P1–I19.
22. Timoshenko SP, Goodier JN: Theory of elasticity. New York: McGraw-Hill, 1987, ch. 1.
23. Hirai S, Tomokuni S: Dynamic modeling of rheological deformation. JSME Conf. on Robotics and Mechatronics Division, 2004, 2A1-H-7.
24. Shames IH, Cozzarelli FA: Elastic and inelastic stress analysis. New Jersey: Englewood, 1992, ch. 4.

Zhongkui Wang

Zhongkui Wang received his B. S. degree and M. S. degree in machine design and theory from Northeast Forestry University, Harbin, China, in 2000 and 2003, respectively. He is currently working on his Ph. D degree in the Department of Robotics at Ritsumeikan University, Japan. His recent research interests include modeling, simulation and parameter identification of rheological objects.

Kazuki Namima

Kazuki Namima received his B. S. degree in robotics from Ritsumeikan University, Japan in 2008. He is currently working on his Master's degree in the Department of Robotics at Ritsumeikan University, Japan. His current research interest is 3D FE simulation of soft-fingered grasping motion.

Shinichi Hirai

Shinichi Hirai received his doctoral degree in applied mathematics and physics from Kyoto University in 1991. He is currently a Professor in the Department of Robotics at Ritsumeikan University. He joined the department in 1996 and was promoted to professor in 2002. His current research interests are modeling and identification of deformable soft objects, realtime computer vision, and soft-fingered manipulation. He is a member of IEEE, RSJ, SICE and JSME.